

# MECHANICAL DESIGN OF A Nb<sub>3</sub>Sn QUADRUPOLE MAGNET

C. Gourdin, A. Devred, M. Durante, M. Peyrot, J.M. Rifflet, P. Védrine  
CEA/Saclay, F-91191 Gif-sur-Yvette, France

## Abstract

One possible application of Nb<sub>3</sub>Sn is the fabrication of short and powerful quadrupole magnets for the crowded interaction regions of large particle accelerators. To learn about Nb<sub>3</sub>Sn technology and evaluate fabrication processes, CEA/Saclay has undertaken a R&D program aimed at designing and building a quadrupole magnet model. After a brief review of the mechanical design, we report on mechanical computations carried out to optimize the magnet straight section.

## 1 INTRODUCTION

The DAPNIA/STCM at CEA/Saclay has undertaken an R&D program to design and build a single-aperture quadrupole magnet model with a Nb<sub>3</sub>Sn Rutherford-type cable. Nb<sub>3</sub>Sn can be used either to achieve a high magnetic field gradient in a large aperture or to permit magnet operation in a sizeable background magnetic flux density. The conceptual design of a 1-m-long, 56-mm-single-aperture Nb<sub>3</sub>Sn quadrupole magnet, with a nominal field gradient of 211 T/m at 11870 A and 4.2 K is presented. Then, we report the main results of FE computations performed to optimize the magnet coil pre-stress. This R&D program is aimed at the final focus system of the TESLA linear collider now under consideration at DESY.<sup>1</sup>

## 2 MAGNET DESIGN

The quadrupole magnet model relies on the same 4-coil and the same conductor geometry as the LHC arc quadrupole magnets.<sup>2</sup> The coils are wound from Nb<sub>3</sub>Sn Rutherford-type cables insulated with quartz fiber tape before being heat-treated and vacuum-impregnated with epoxy resin. The cable is developed in collaboration with Alstom/MSA/Fil<sup>3</sup> while an evaluation program of different insulation systems has led to the selection of a quartz fiber tape.<sup>4</sup> The Lorentz forces are restrained by laminated, 2-mm-thick, austenitic steel collars locked around the coils by means of tapered keys. The collared-coil is centered within a precisely-machined, steel inertia tube which delimits the region of liquid helium circulation. A cross-sectional view of the quadrupole magnet model is shown Fig. 1.

The objectives of the mechanical design are : (1) all parts of coils should remain in compression at nominal current, and (2) peak stress in coils should be less than 150 MPa at all time.

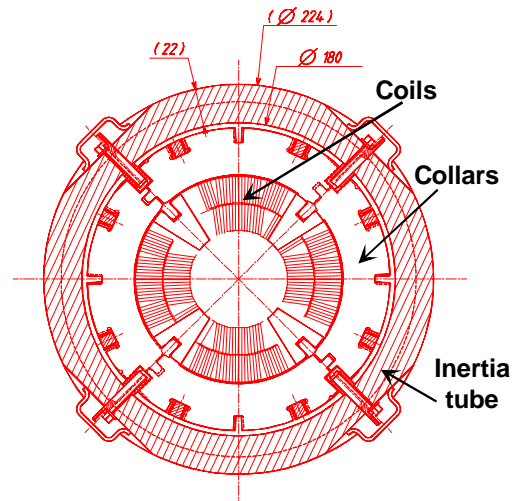


Figure 1 : Cross Sectional View of Quadrupole Magnet Model

## 3 OPTIMIZATION OF MECHANICAL MODEL

### 3.1 Model description

The 2D cross-section of the collared-coil assembly is modeled using the CASTEM2000 Finite Element analysis software package.<sup>5</sup>

The coils are made up of six components:

- Nb<sub>3</sub>Sn conductor packages,
- angular wedges,
- interlayer insulation,
- ground insulation,
- interpole insulation,
- pole wedges (with a keyway).

Two half coils are used in the FE model.

The coil support system is made up of 4 components: front and back collars, tapered keys and sliding strips. The back and front collars are used to model the 3D-effects of the lamination stacking in alternated layers. The purpose of the sliding strips is to facilitate key insertion into collar keyways.

Boundary conditions are imposed on the coil symmetry planes, and on the back and front collar symmetry planes. Frictional Contact elements (six contact surfaces) are used between coils and collars (back and front), and between tapered keys and sliding strips. All surfaces are assumed to be frictionless to reduce model size and computing time.

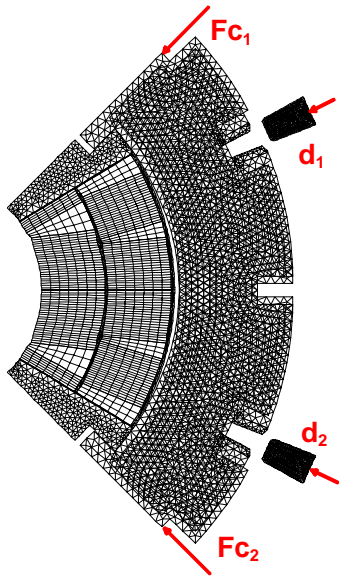


Figure 2 : Initial Mesh Used for Stress Analysis

The mesh used for stress analysis counts 8796 elements and is shown Fig. 2. The number of degrees of freedom was about 12000.

### 3.2 Material Properties

Table 1 lists the thermal and mechanical properties of the different materials used in the FE model, which are assumed to be isotropic. Thermo-mechanical properties of Nb<sub>3</sub>Sn conductor package (including tape and resin) have been measured using ten-stack samples<sup>6</sup> fabricated according to processes similar to those foreseen to be used for real coils.

### 3.3 Loading

Mechanical loading is divided into four successive parts corresponding to the history of magnet loading:

- (1) pre-collaring with bars, (2) collaring with keys, (3) cool down to 4.2 K, (4) excitation to 11870 A.

The pre-collaring process is modeled by applying forces onto the bottom of the collar keyways along the pole axes ( $F_{c1}$  and  $F_{c2}$  in Fig. 2). Then, radial displacements are imposed on the two tapered keys to simulate the collaring process ( $d_1$  and  $d_2$  in Fig. 2).

The temperature distribution throughout cool-down is assumed to be uniform.

The Lorentz forces induced during energization are computed using the ROXIE analysis software.<sup>7</sup>

The average components of the Lorentz forces over a coil octant at 11870 A are:  $F_x = 400$  kN/m and  $F_y = -711$  kN/m.

Table 1 : Thermal and Mechanical Properties

Material Components	Temp. K	Young Modulus GPa	Integrated Thermal Expansion
Steel 13Rm19	300	210	
Collars & Keys	4.2	210	$-2.9 \cdot 10^{-3}$
Copper Alloy	300	110	
Wedges	4.2	110	$-3.6 \cdot 10^{-3}$
Insulation	300	4	
	4.2	4	$-6.0 \cdot 10^{-3}$
Nb <sub>3</sub> Sn + tape + resin Conductor package	300	30	
	4.2	42	$-3.9 \cdot 10^{-3}$

### 3.4 Results

The stresses and deformations are calculated following the assembly sequence: (1) pre-collaring, (2) collaring, (3) cool down and (4) energization. Optimized results are summarized in Table 2. The various points where stresses or displacements are reported are indicated in Fig. 3, along with the collared-coil deformation at nominal current.

#### Pre-collaring and collaring

During pre-collaring with bars, the azimuthal coil stress is small ( $< 52$  MPa). The main goal of this process is to put all parts in good position before full collaring.

The room temperature pre-stress is imposed by the insertion of tapered keys. Several computations were carried out to study the influence of coil size on pre-stress and on the force required for the collaring press.

The optimized azimuthal coil stress at the end of collaring is shown Fig. 4. The peak stress is less than 142 MPa.

#### Cool down

During cool down, the azimuthal coil stress decreases by 20 MPa in average, because of the thermal shrinkage differential between collars and coils (see Table 1).

#### Excitation

At 11870 A, all parts of coils remain under compression and the peak stress is 134 MPa.

## CONCLUSIONS

The stress in the coils decreases during cool-down and energization. All parts of coils remain in compression at nominal current. The peak stress in the coils is less than 150 MPa at all time.

The FE computation results validate the main features of the mechanical design.

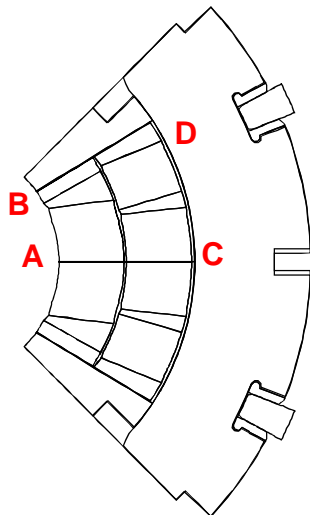


Figure 3 : Collared-Coil Deformation at 11870 A

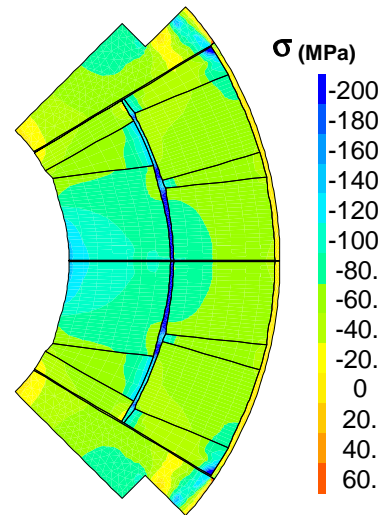


Figure 4 : Azimuthal Coil Stress Distribution at 11870 A

Table 2 : Selected Results of Mechanical Computations

	Units	Collaring with bars	Collaring with keys	Cool down	Energization				
<b>Conditions</b>									
Temperature	K	300	300	4.2	4.2				
Current	A	0	0	0	11870				
Load on bars	N/mm	280							
Load on keys	N/mm		<b>891</b>						
<b>Coils</b>									
Stress		$\sigma_\theta$	$\sigma_r$	$\sigma_\theta$	$\sigma_r$	$\sigma_\theta$	$\sigma_r$	$\sigma_\theta$	$\sigma_r$
Point A	MPa	<b>-52</b>	-9	<b>-142</b>	-31	<b>-119</b>	-25	<b>-134</b>	-31
Point B	MPa	-2	0	-87	-2	-52	-3	<b>-13</b>	0
Point C	MPa	-2	0	-47	-19	-34	-7	-41	-10
Point D	MPa	-29	-7	-111	-58	-82	-28	-75	-25
Average over first layer	MPa	-27	-4	-102	-20	-78	-10	-77	-16
Average over second layer	MPa	-16	-2	-76	-34	-57	-20	-60	-25
Average over coil	MPa	-21	-3	-87	-28	-66	-16	-67	-21
Displacement		$\Delta_\theta$	$\Delta_r$	$\Delta_\theta$	$\Delta_r$	$\Delta_\theta$	$\Delta_r$	$\Delta_\theta$	$\Delta_r$
Average over midplane	mm		-0.009		-0.06		-0.248		-0.243
Average over pole plane	mm	-0.004	-0.026	-0.012	-0.085	-0.009	-0.267	-0.010	-0.266
<b>Collars</b>									
Peak Von Mises Stress	MPa			522				<b>1440</b>	

## REFERENCES

- [1] R. Brinkmann, et al., "A new beam delivery system (BDS) for the TESLA linear collider," presented at this conference.
- [2] M. Peyrot, et al., "Construction of the new prototype of main quadrupole cold mass for the arc short straight sections of LHC," IEEE Trans. Appl. Supercond., Vol. 10 No. 1, pp. 170-173, 2000.
- [3] M. Durante, et al., "Development of a Nb<sub>3</sub>Sn multifilamentary wire for accelerator magnet applications", Presented at ICMC2000, Brazil , 2000.
- [4] A. Devred, et al., "Insulation systems for Nb<sub>3</sub>Sn accelerator magnet coils fabricated by the *wind and react* technique," Advances in Cryogenic Engineering (Materials), Vol. 46, pp.143-150, 2000.
- [5] CASTEM, trademark from CEA/Saclay, France.
- [6] P. Védérine et al., "Measurement of the thermo-Mechanical properties of NbTi Windings for accelerator magnets," IEEE Trans. Appl. Supercond., Vol. 9 No. 2, pp. 236-239, 1999.
- [7] S. Russenschuck, et al., "Integrated design of superconducting accelerator magnets. A case of study of the main quadripole", The European Physical Journal, AP 1, pp. 93-102, 1998.